**Kingdom of Saudi Arabia**
**Imam Mohammad bin Saud Islamic**
**University College of Science**
**Chemistry Department**

# Simple preparation of $ZnAl_2O_4$, 2.5%$NiO/ZnAl_2O_4$, and 5%$NiO/ZnAl_2O_4$ composites for efficient water treatment

*Research submitted as partial fulfillment of the requirements for the completion of the BSc Degree in Chemistry*

**By**

**Abdullah Majed Abdullah Almajed**

**&**

**Yousef Saud Matar Alshammari**

## Supervisor

**Dr. Faisal K. Algethami.**

**Dr. Babiker Y. Abdulkhair**

**October - 2024**

# *Acknowledgement & Dedication*

***Our heartfelt gratitude goes to our supervisors, for all of their help and guidance.***

***Please accept our heartfelt gratitude for the chemistry faculty's hard work.***

***This endeavor is in honor of our loved ones, who have always supported us and inspired us to keep going.***

## Figures

## Abstract

This work generated ZnAl2O4, 2.5%NiO/ZnAl2O4, and 5%NiO/ZnAl2O4 composites using a one-put rapid approach. Studied composites for BF and water adsorption. Doping ZnAl2O4 with NiO increased its sorption capacity and yielded qt values of 158.1, 178.3, and 197.2 mg g-1. Fast treatment sorbents achieved over 90% of their qt values in 20–30 minutes, and all sorption processes reached equilibrium at 60 minutes. The rate-order output of BF removal showed that BF sorption on ZnAl2O4 and 2.5%NiO/ZnAl2O4 fit the PS model better than the PF model. The rate-control output of BF removal showed that the LF controlled ZnAl2O4 and 2.5%NiO/ZnAl2O4 sorption. IP model controlled BF sorption on 5%NiO/ZnAl2O4.

# الملخص باللغة العربية

في هذا العمل تم إنتاج مركبات ZnAl2O4 و2.5%NiO/ZnAl2O4 و5%NiO/ZnAl2O4 باستخدام طريقة سريعة أحادية. تمت دراسة المركبات لامتزاز BF من الماء. أدى تطعيم ZnAl2O4 بأكسيد النيكل إلى زيادة قدرته على الامتزاز وأسفر عن سعة امتزاز بالقيم: 158.1 و178.3 و197.2 مجم/جم. حققت المواد المازة معالجة سريعة بامتزاز أكثر من 90% من قيم المادة الملوثة في 20-30 دقيقة، ووصلت جميع عمليات الامتصاص إلى التوازن في 60 دقيقة. أظهر الناتج ان معدل إزالة BF أن متزاز BF على ZnAl2O4 و2.5%NiO/ZnAl2O4 يناسب نموذج PS بشكل أفضل من نموذج PF والعكس صحيح بالنسبة ل 5%NiO/ZnAl2O4 . أظهر التحقيق في ميكانيكية التحكم في إزالة BF أن LF يتحكم في امتزاز ZnAl2O4 و 2.5٪ NiO / ZnAl2O4. بينما يتحكم نموذج IP في امتزاز BF على 5%NiO/ZnAl2O4.

# Chapter One

## Introduction
## and Literature Review

# 1. Introduction

## 1.1. Preparation of nanomaterials

Researchers in a variety of disciplines have made heavy use of nanoscale particles in recent years. The capacity to modify these materials and increase their accessibility, however, has led to a recent upturn in interest [1]. Numerous fields make use of nanoscale materials, including electronics, biology, medicine, cosmetics, ecology, materials science, magnetism, and environmental science. The enormous potential of nanotechnology has prompted a worldwide upsurge in funding for related research and development. Both the amount of time and money spent on nanotechnology research has increased significantly since 1999. Greater social advancement and sustainable development are the primary goals of the researchers. If we can understand the steps involved in making nanoparticles, like those in combustion systems, we can come up with efficient ways to reduce the amount of pollutants and the amount of pollution they cause [2]. The bottom-up synthesis of nanomaterials involves combining atoms and molecules into molecules on the nanoscale. Methods for preparing nanomaterials include, and the second viewpoint is top-down, which involves reducing bulk materials to the nanoscale [3-5].

### 1.1.3. Sol-gel method

A popular nanomaterials approach is the sol-gel procedure. A surfactant or nonaqueous solvent controls particle size in a suitable solvent during precursor reaction. In a liquid media, the particles prevented tiny crystals from clumping.

Several famous chemists studied the periodic preBFitation events that caused Liesegang rings and gel crystal formation [4, 6, 7]. This phenomenon has spurred much descriptive research. Roy and colleagues took advantage of chemical homogeneity in colloidal gels. They improved them, allowing the sol-gel method to synthesize numerous ceramic oxide compositions containing Al, Si, Ti, Zr, etc. previously unreachable using ceramic powder methods. [8, 9]. The starting water and ammonia content, precursor, solvent, and reactant temperature determine the final spherical particle size. [10, 11].

### 1.1.1. Solvothermal method

One of the most environmentally friendly and promising synthesis methods, the solvothermal (hydrothermal) approach, uses aqueous or nonaqueous solvents to optimize particle size distribution and shape control. This technique homogenizes metal salts and adjusts the medium pH to alkaline with a basic solution. The target nanomaterial controls the homogenized solution's thermal treatment temperature and time. Time, temperature, medium, and precursors affect nanoparticle size and shape [12].

### 1.1.2. De-emulsification

Using a salting-out reagent and colloidal stabilizer, an aqueous gel dissolved the polymer and medication to create an emulsion. This method is suitable for thermally unstable materials since it does not require a temperature increase. Salting-out agents included magnesium, calcium, sodium sulfate, and sodium chloride. We also employed sucrose and other non-electrolytes. Some situations require a colloidal stabilizer like ethyl cellulose or polyvinylpyrrolidone. Diluting the organic solvent-water emulsion with extra water increases nanomaterial production. Wash the product to remove the stabilizer and salting agent [13].

### 1.1.4. Green synthesis

In green nanomaterial manufacturing, capping substrates might be plant extracts or microorganisms. Plant-based nanoparticles are mass-produced for biosynthesizing. Plants produce metallic nanoparticles from seeds, leaves, stems, roots, and latex. The safest technique to make nanoparticles was eco-friendly. The need for green metallic nanoparticle production has grown. We want to eliminate synthetic waste, chemical byproducts, and derivative substrates. Biomaterials from nature are useful for eco-friendly nanoparticle manufacturing. Scientists use bacteria, algae, fungi, and plants to make cheap, energy-efficient, and environmentally friendly metal nanoparticles. Green synthetic methods are replacing physicochemical ones in the industry [14, 15].

## 1.2. Water pollution

Water is crucial to human survival since water quality decline affects all life. Organic pollutants in water systems globally are a problem. Due to their widespread use and market demand, pharmaceuticals and chemical dyes are frequently used in water and sewage systems [16, 17]. The quality of drinking water has harmed public health. Water contamination causes most waterborne illnesses, decimating urban populations. Due to this, people must drink untreated irrigation water, which has serious health consequences [16]. Understanding water pollutants' sources, interactions, and effects is essential to reducing their environmental impact and preserving ecosystems. The inappropriate disposal of aging pollutants, decontaminating equipment, and eradicating poorly manufactured and contaminated human and animal waste commodities might introduce such pollutants into water systems [17-19]. Dangerous aquatic pollution makes industrialized nations' water supply systems vulnerable. The US has more water than its rivers and lakes generate. Chemically hazardous groundwater may exist in some areas. Water pollutants include heavy metals, chlorinated hydrocarbons, organic pigments, industrial metal plating, and bacteria. Since World War II, synthetic chemical production and use have increased. The presence of these pollutants has contaminated water supplies. Examples include pesticide use, agricultural runoff, and improper industrial rubbish disposal into waterways. Incorrect chemical waste disposal in landfills, storage lagoons, treatment ponds, and other facilities can contaminate groundwater. Pollution and unequal distribution limit the usability of many global water sources, which appear infinite. Water scarcity affects many people worldwide, causing many wars. Groundwater, obtained by drilling, excavation, or springs, greatly influences river baseflow. Nearly 80% of ocean contaminants come from land-based sources, usually industrial operations or indirect dumping of human waste [20-22].

The Netherlands monitored the entire nation from 2010 to 2014. The operation detected high pesticide levels in groundwater wells, which is alarming. This study tested shallow groundwater samples from the Netherlands and Flanders for 405 compounds and 52 metabolites. The results showed neonicotinoids, which are mobile and persistent, at 0.12–0.01 g/L [23]. The Yangtze River Basin in Hubei Province, Central China, had high organochlorine and organophosphate pesticide levels. Sixteen groundwater samples from the given area contained fifteen organochlorines and four organophosphates. The four organophosphate pesticides' mean values were 196.01 ng/L for aldrin, dieldrin, and hexachlorocyclohexane. The water supply did not meet EPA criteria [24]. The phreatic aquifer beneath the Pampean area of Argentina contains organochlorine pesticides, indicating their long-term existence. Certain areas have high groundwater fluoride levels, according to multiple research. Avoid using groundwater with high fluoride contents for long durations. The health benefits of fluoride justify fluoridating public water sources. However, excessive fluoride absorption can cause dental and skeletal fluorosis. This study found that neonates and toddlers are more sensitive to dental fluorosis, a noncarcinogenic risk. A recent groundwater fluoride investigation in Agra City, India, found a wide range of amounts over the WHO 1.5 mg/L standard. The average fluoride concentration in 51 groundwater samples from Siddipet Vagu, India, was 3.7 ppm. 51% of samples exceeded the WHO safety standard of 1.5 mg/L for fluoride [25]. The study examined fifty borehole samples from intensive agriculture areas on the West Bank of the Nile River in Luxor Governorate, Egypt, and found that 62% were moderately vulnerable to groundwater pollution and 38% were high. Nitrate pollution from nitrogen-based fertilizers has poisoned 52% of the land. Recent research found that Chungcheong Province, South Korea, had a mean nitrate concentration of 12.4 mg/L [26]. Groundwater, oceans, and rivers contain pharmaceutical pollutants (PhCs) worldwide. Explaining humanity's dire situation may help: 50% of Earth's water has been poisoned since 1970. The US acknowledged PhC-polluted water as a public health risk in 1999 [27-30]. Over half of China's population drank polluted water during the same period. Indian rivers, groundwater, and water treatment facilities contain PhCs. These substances can reach 31.0 mg $L^{-1}$ [31, 32]. The need for infectious disease treatments and growing agricultural, poultry, and cattle output drive PhC pollution . The most representative tetracyclines include tigecycline, chlortetracycline, tetracycline (OXTC), and d cycline [33]. Antibiotics and food preservatives have increased tetracycline (TC) use. Multiple studies have found TCs in soil and water reservoirs in the US, UK, and China [34]. The growth of PhCs in seas, oceans, rivers, and drinking water sources demonstrates that current treatment approaches are ineffective [35-43]. Thus, PhC prevention requires new methods. Nanomaterials have advanced the adsorption process, which removes non-degradable water contaminants like heavy metals. This procedure is simple, energy-efficient, and does not release harmful fragments

### 1.3. Aim of the study

This study aimed to prepare $ZnAl_2O_4$, 2.5%NiO@$ZnAl_2O_4$, 5%NiO@$ZnAl_2O_4$, and 10%NiO@$ZnAl_2O_4$ triple composite as environmentally safe sorbents. A one-put route was adopted in order to simplify the process. The prepared double and triple composites will be tested for removing organic pollutants exampled by BF, and their sorption kinetics will be investigated.

# Chapter Two

## Materials and Methods

## 2. Materials and methods

### 2.1 Materials

BF and Nickel acetate were provided from Fluka, USA. D(+)-Glucose monohydrate (GL) was provided from Riedel-de-Haen, Germany. Zinc nitrate hexahydrate and aluminum chloride hexahydrate ($AlCl_3$-$6H_2O$) were purchased from (LOBA CHEMIE, Mumbai, India).

### 2.2. Preparation of $ZnAl_2O_4$

15.306 g of $Zn(NO_3)_2$, 11.813 g of $ACl_3$, and 10 g of GL were transferred to a 500 mL beaker. About 15 mL of distilled water was added. The mixture was turned into a clear solution by heating on a hotplate (120°C), then the hotplate temperature was raised (250°C) until the GL was carbonized. The obtained powder was grinned, transferred to a porcelain dish, and calcined at 600°C for 3.0 h. The process was repeated using the typical Al-Zn amounts with the addition of a proper amount of Nickel acetate to obtain 2.5%NiO@$ZnAl_2O_4$, and 5% NiO@$ZnAl_2O_4$.

### 2.3. Preparation of BF and solutions

0.1g of BF was weighed using an analytical balance and transferred to a 1L volumetric flask to obtain 100 mg $L^{-1}$ BF solution. Then, 600 mL of DW was added to the flask and put into an ultrasonic path. The DW completed the resulting solution to the neck mark.

### 2.4. Adsorption

0.05g of each sorbent ($ZnAl_2O_4$, 2.5%$NiO/ZnAl_2O_4$, and 5% $NiO/ZnAl_2O_4$) was measured in a separate 150 mL beaker. 100 mL of the 100 mg $L^{-1}$ BF solution was poured into each beaker. A portion of the mixture was withdrawn till the BF sorption reached the equilibrium. The aliquots were filtered via a 0.22μm syringe filter, and the absorbance was measured utilizing a UV-Vis-spectrophotometer ($\lambda_{max}$ = 550 nm).

# Chapter Three

## Results and Discussion

## 3. Results and discussion

### 3.1. Contact time study

The contact time study of BF and sorption onto the as-prepared $ZnAl_2O_4$, 2.5%$NiO/ZnAl_2O_4$, and 5%$NiO/ZnAl_2O_4$ were studied. The BF and absorbance measured during the study were employed for calculating their remaining concentrations (unadsorbed) at each time interval via Eq. 1. Using Eq. 2 was utilized to calculate the adsorption capacity at each period (the BF or milligrams adsorbed onto one gram of sorbent, $q_t$, mg $g^{-1}$).

$$C_t = \frac{Absorbance_{sample}}{Absorbance_{standard}} \times conc._{standard} \qquad (1)$$

$$\mathrm{q_t} = \frac{(\mathrm{C_o} - \mathrm{C_t})\,\mathrm{V}}{\mathrm{m}}, \qquad (2)$$

Fig. 1, 2, 3, and 4 demonstrate the adsorption trend of BF onto $ZnAl_2O_4$, 2.5%$NiO/ZnAl_2O_4$, 5%$NiO/ZnAl_2O_4$, and a comparison between the three sorbents, respectively. The $ZnAl_2O_4$, 2.5%$NiO/ZnAl_2O_4$, and 5%$NiO/ZnAl_2O_4$ showed $q_t$ values of 158.1, 178.3, and 197.2 mg $g^{-1}$, respectively,these results reflected that doping $ZnAl_2O_4$ by NiO improved the sorption ability of the $ZnAl_2O_4$. Notably, almost 90% of the gained $q_t$ values were acquired within the first 20 to 30 minutes, and all sorption processes reached equilibrium at 60 minutes, which indicated a fast treatment sorbents.

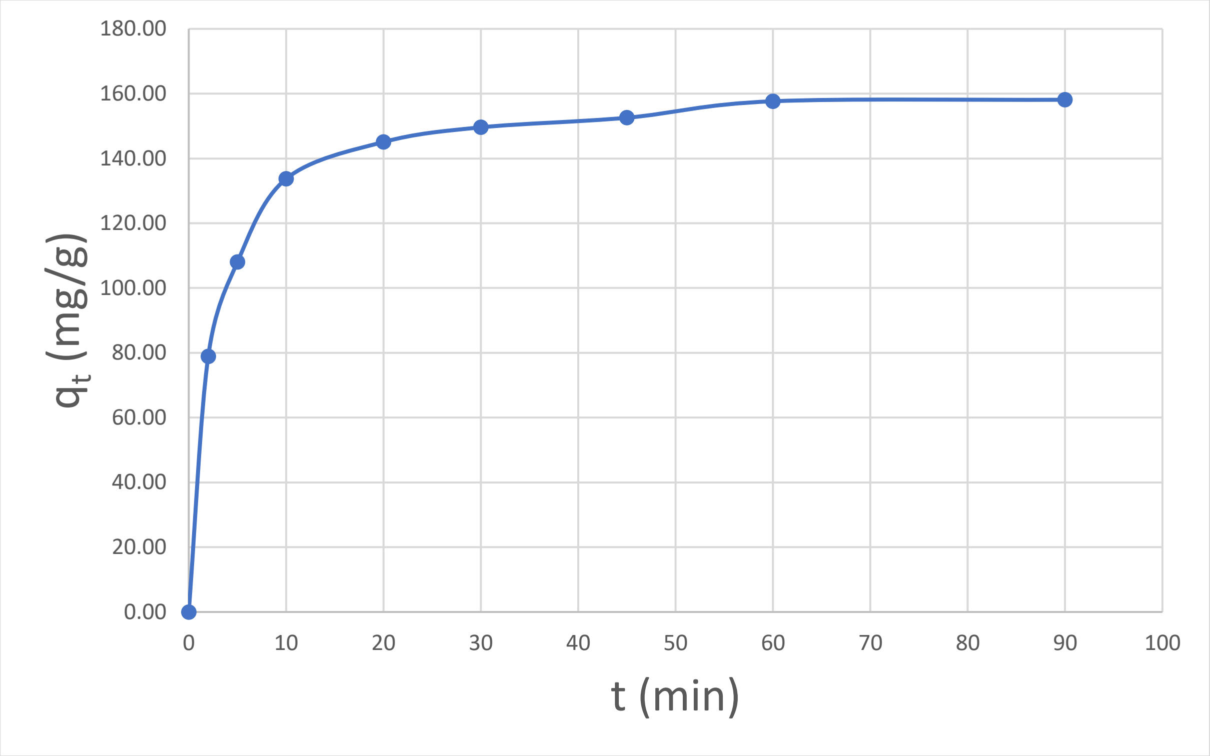

**Fig. 1 The contact time trend of BF sorption onto the $ZnAl_2O_4$ nanocomposite.**

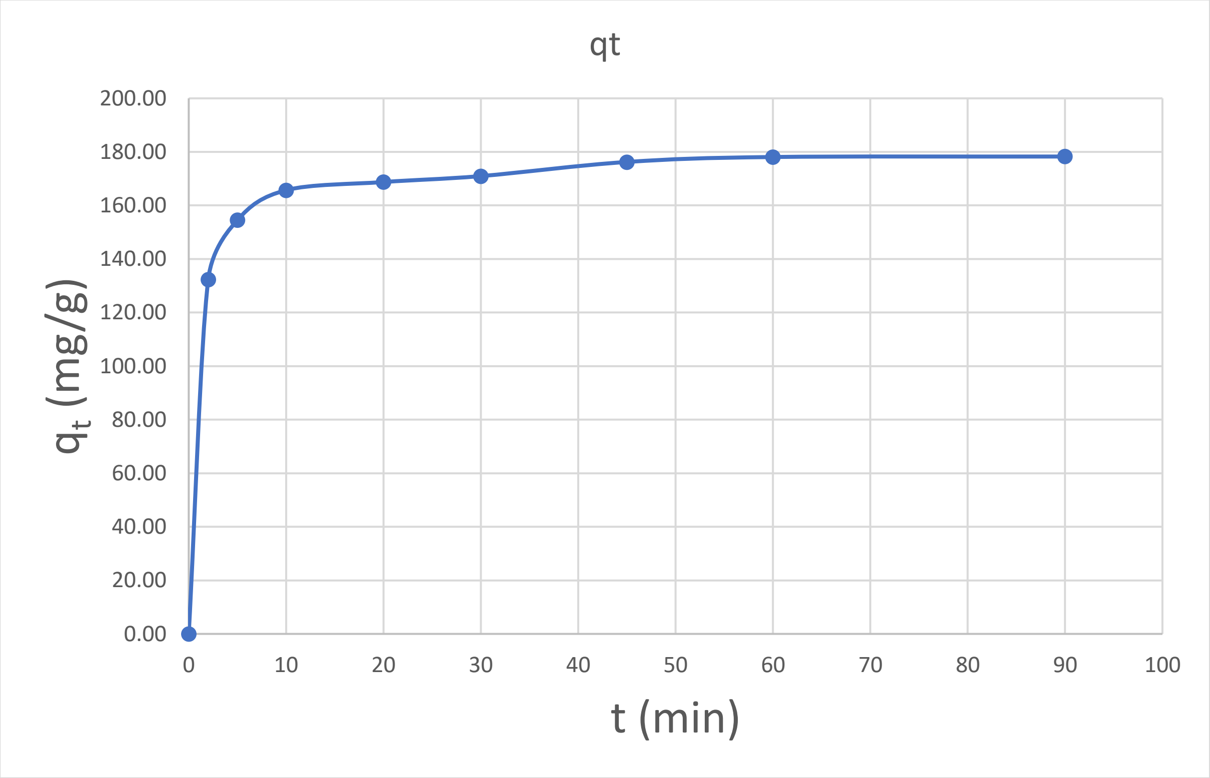

**Fig. 2 The contact time trend of BF sorption onto the 2.5%$NiO/ZnAl_2O_4$ composite.**

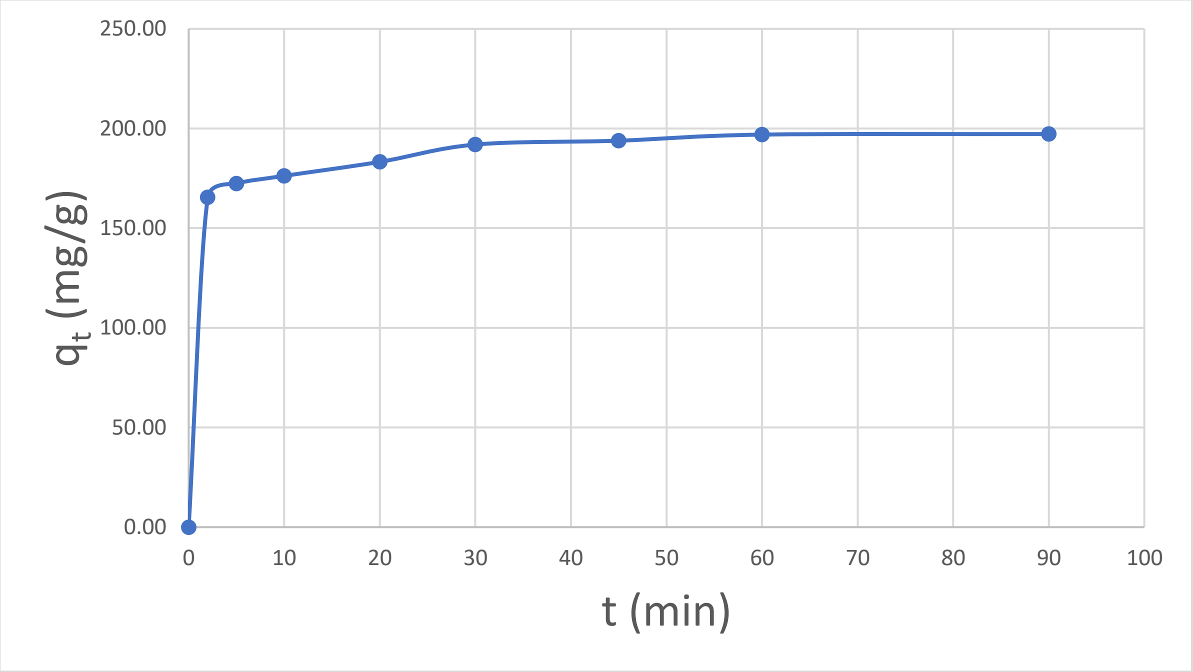

**Fig. 3 The contact time trend of BF sorption onto the 5%NiO/$ZnAl_2O_4$ composite.**

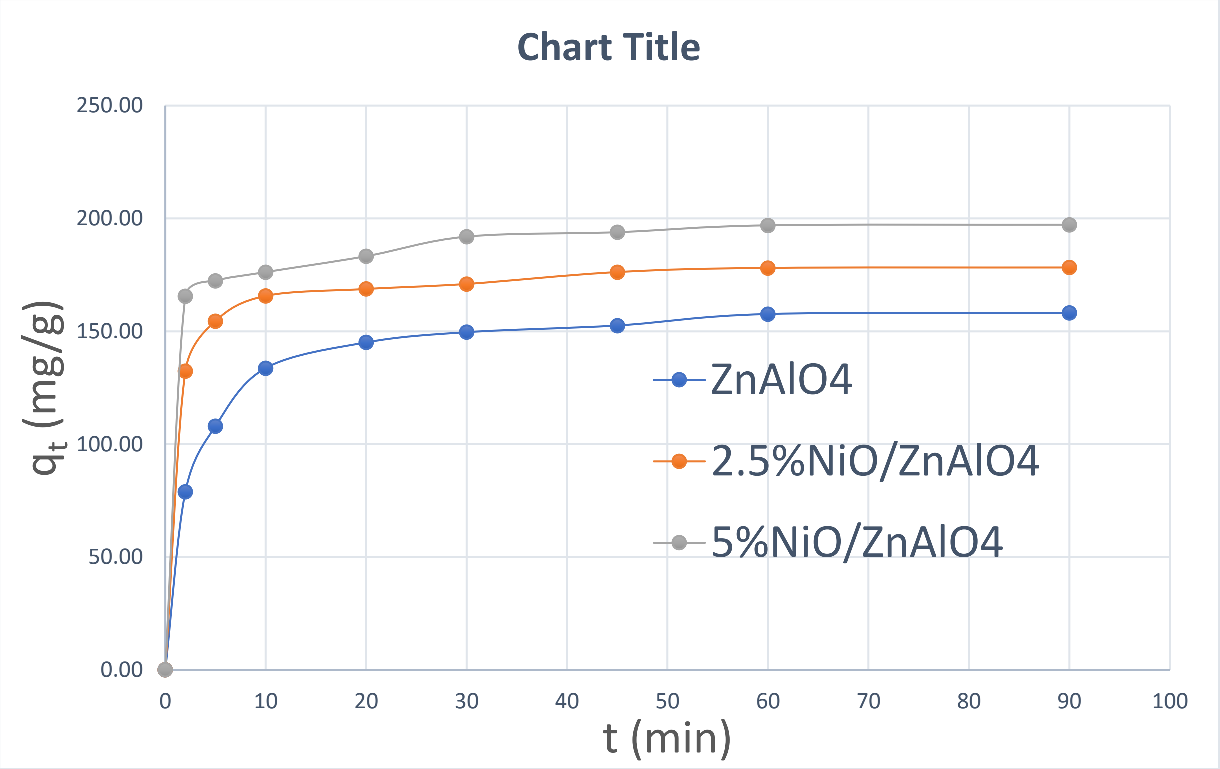

**Fig. 4 The contact time trend of BF sorption onto** $ZnAl_2O_4$, 2.5%NiO/$ZnAl_2O_4$, and 5%NiO/$ZnAl_2O_4$ **composite.**

### 3.2 Adsorption rate order

The adsorption rate order of BF and removal by $ZnAl_2O_4$, 2.5%NiO/$ZnAl_2O_4$, 5%NiO/$ZnAl_2O_4$, and 10%NiO/$ZnAl_2O_4$ was studied via pseudo-first-order (PF, Eq. 3) and pseudo-second-order (PS, Eq. 4) kinetic models.

$$\ln(q_e - q_t) = \ln q_e - k_1 . t \qquad (3)$$

$$\frac{1}{q_t} = \frac{1}{k_2 . q_e^2 \, t} + \frac{1}{q_e} \qquad (4)$$

The symbol $q_e$ (mg g-1) represents the equilibrium adsorption capacity. The PF and PS constants are also time-dependent, with the former represented as k1 ($min^{-1}$) and the latter as k2 (g $mg^{-1}$ $min^{-1}$). The PF plots of the BF adsorption onto $ZnAl_2O_4$, 2.5%NiO/$ZnAl_2O_4$, and 5%NiO/$ZnAl_2O_4$ composites were depicted in Fig. 5, 6 and 7, respectively. Additionally, Fig.8, 9, and 10 illustrated the PS plots of BF sorption onto $ZnAl_2O_4$, 2.5%NiO/$ZnAl_2O_4$, and 5%NiO/$ZnAl_2O_4$, respectively. The rate-order output of BF removal (Table 1) illustrated that the sorption on $ZnAl_2O_4$, and 2.5%NiO/$ZnAl_2O_4$ showed better fitting to the PS model, conversely, BF sorption onto the 5%NiO/$ZnAl_2O_4$ fitted the PF model.

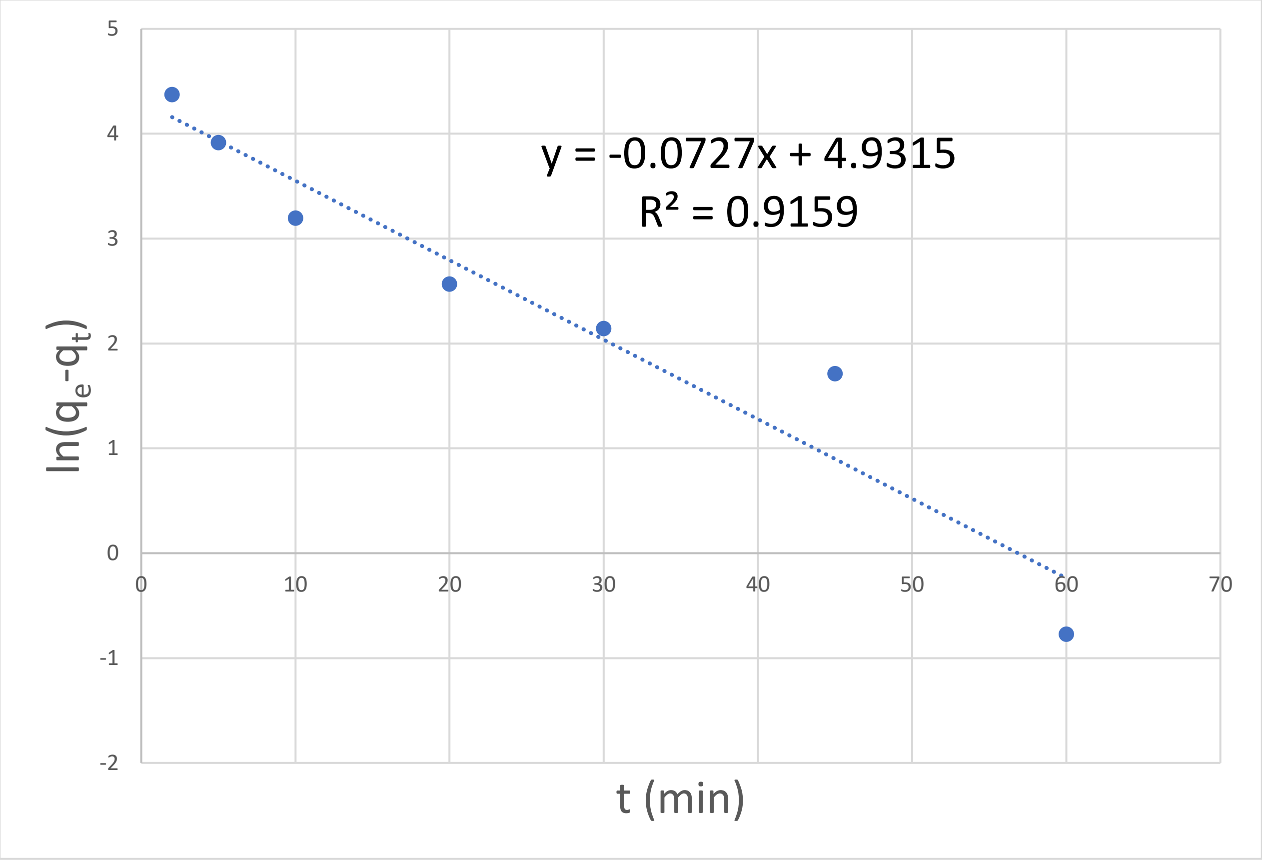

**Fig. 5 The PF investigation of BF sorption onto $ZnAl_2O_4$ composite.**

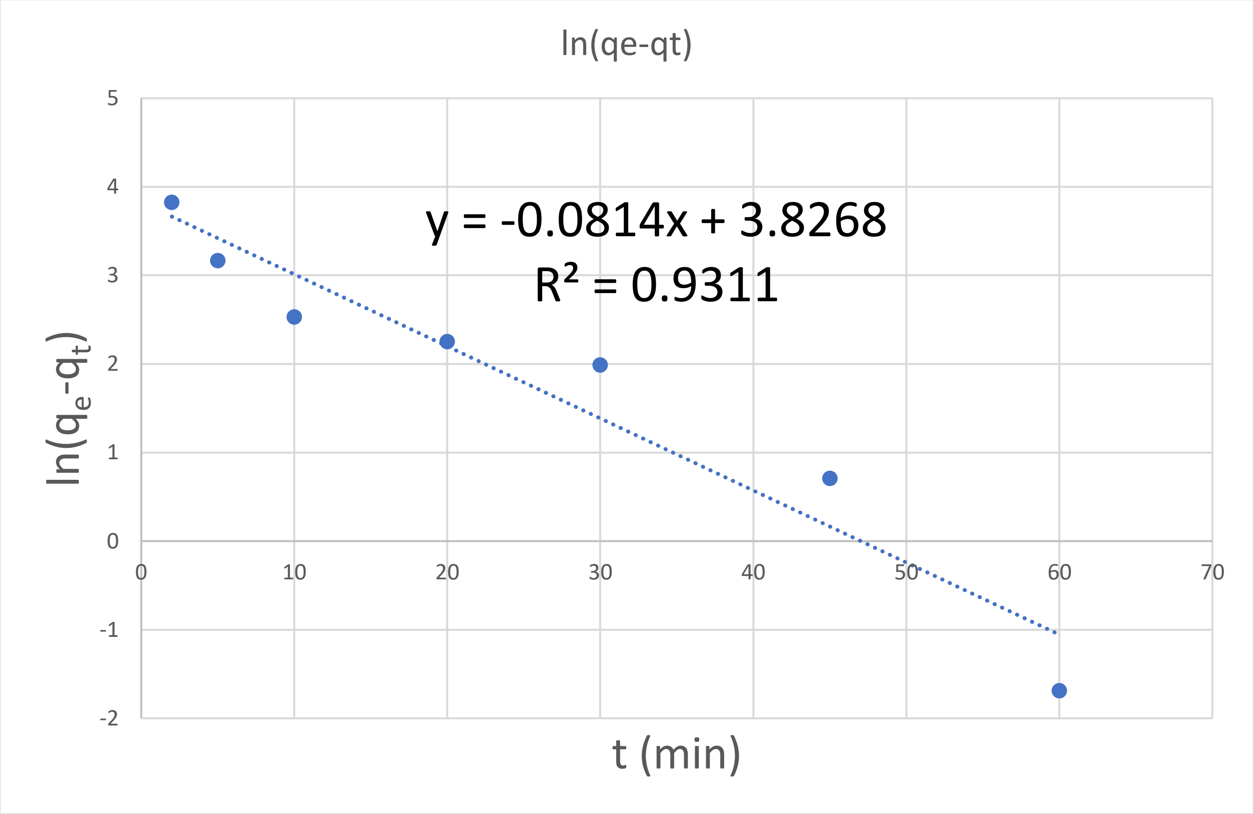

**Fig. 6 The PF investigation of BF sorption onto 2.5%NiO/$ZnAl_2O_4$ composite.**

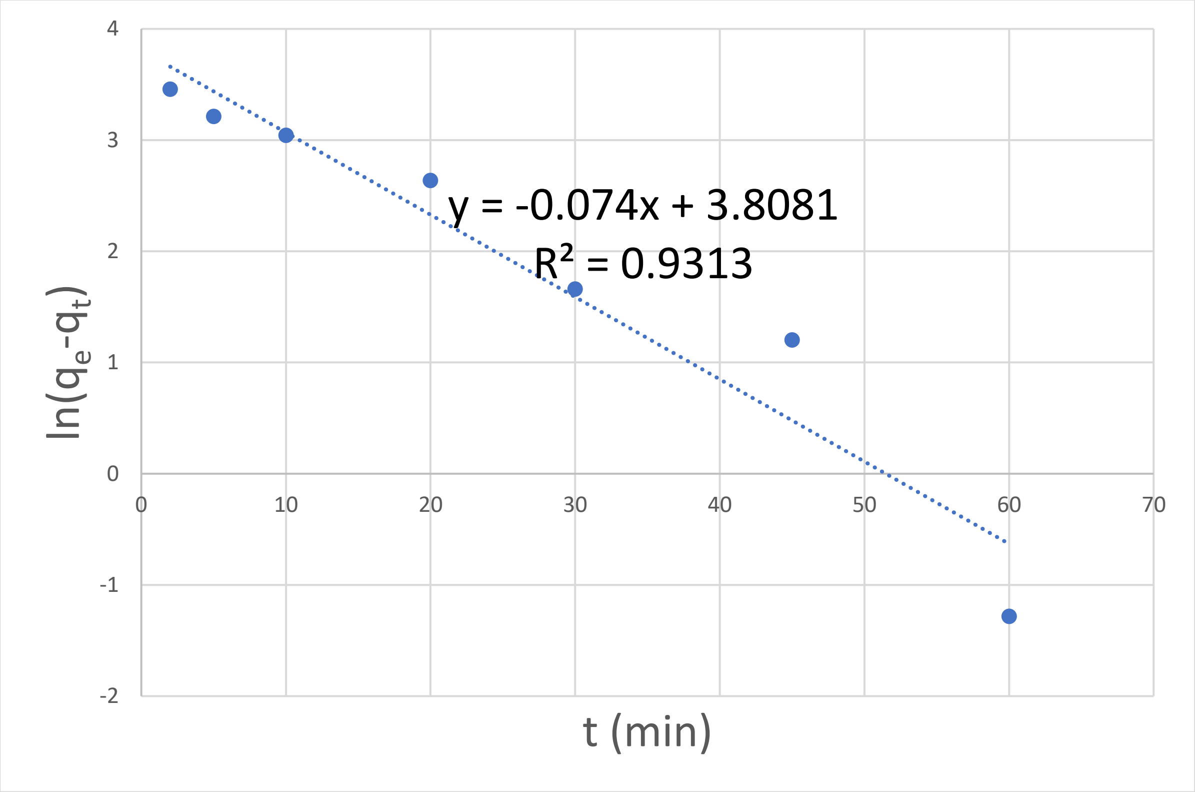

**Fig. 7 The PF investigation of BF sorption onto 5%NiO/$ZnAl_2O_4$ composite.**

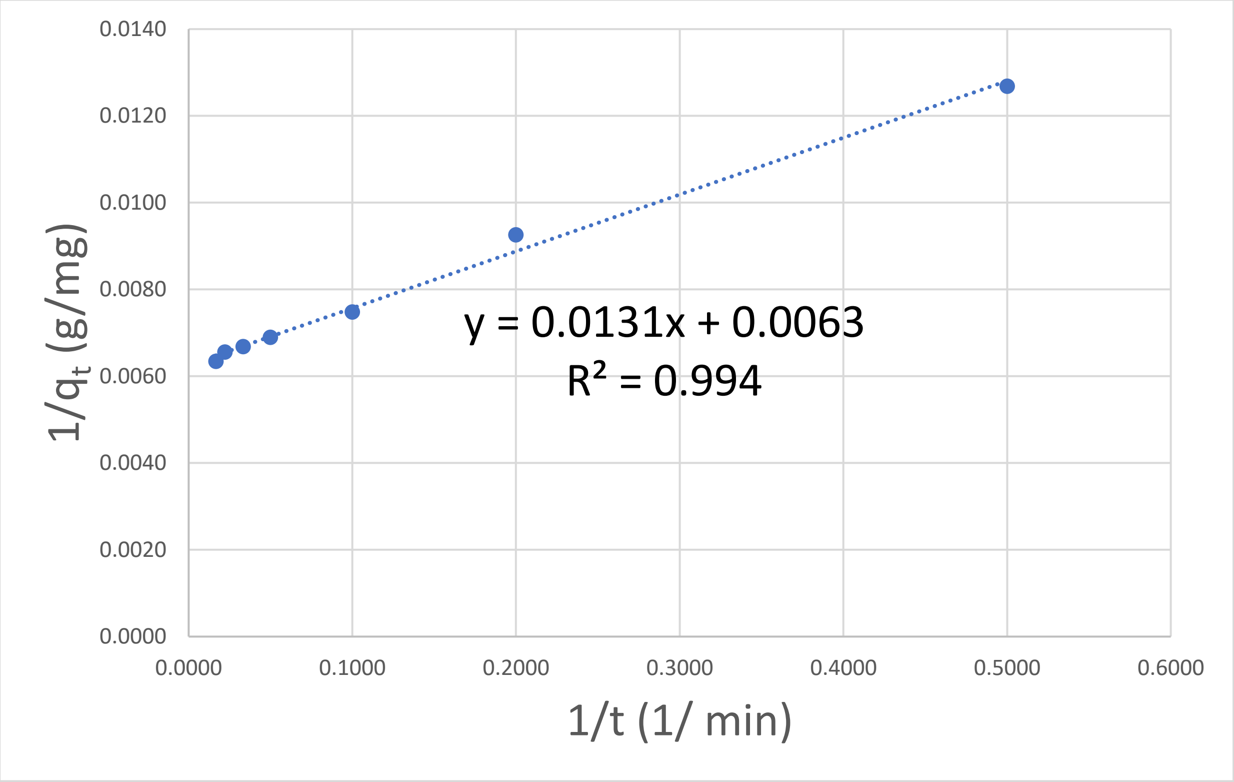

**Fig. 8 The PS investigation of BF sorption onto $ZnAl_2O_4$ composite.**

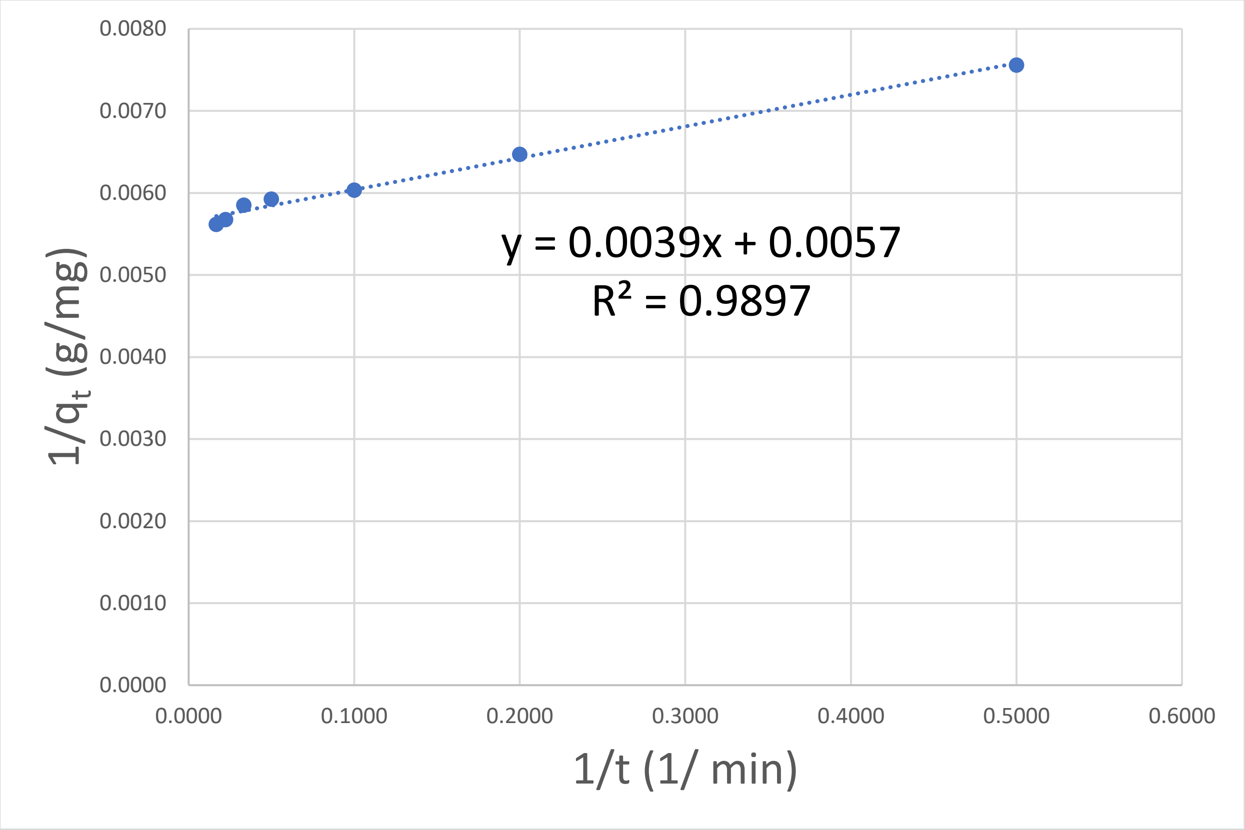

**Fig. 9 The PS investigation of BF sorption onto 2.5%NiO/$ZnAl_2O_4$ composite.**

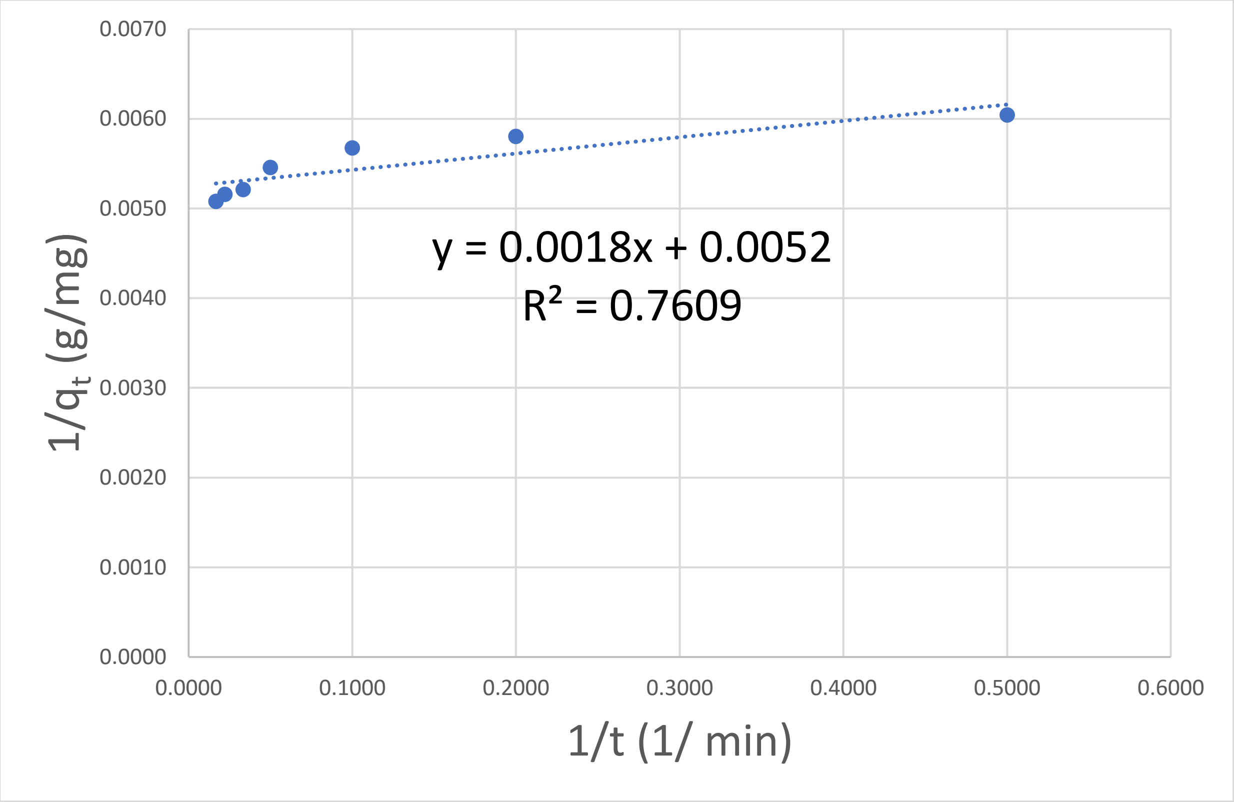

**Fig. 10 The PS investigation of BF sorption onto 5%NiO/$ZnAl_2O_4$ composite.**

**Table 1 The adsorption rate order results of BF removal by $ZnAl_2O_4$, 2.5%NiO/$ZnAl_2O_4$, 5%NiO/$ZnAl_2O_4$.**

| Adsorbent | qe exp. (mg $g^{-1}$) | *PFO* | | *PSO* | |
|---|---|---|---|---|---|
| | | $R^2$ | $k_1$ | $R^2$ | $k_2$ |
| $ZnAl_2O_4$ | 158.11 | 0.9321 | 0.0758 | 0.9940 | 0.00299 |
| 2.5%NiO/ $ZnAl_2O_4$ | 178.27 | 0.9311 | 0.0814 | 0.9897 | 0.00828 |
| 5%NiO/ $ZnAl_2O_4$ | 197.23 | 0.9313 | 0.0740 | 0.7609 | 0.01513 |

### 3.3 Adsorption control mechanism

It is believed that there are two steps to the adsorption process, the first of which is the movement of adsorbate molecules from a liquid to a solid sorbent surface. Step two involves getting the sorbate molecules to go deep into the sorbent. The rate control mechanism, the slowest sorption step, determines the adsorption rate. The rate-control mechanism of BF and removal by $ZnAl_2O_4$, 2.5%$NiO/ZnAl_2O_4$, and 5%$NiO/ZnAl_2O_4$ was studied using the intraparticle (IPD, Eq. 5) and the liquid-film (LFD, Eq. 6) diffusion model.

$$q_t = K_{IP} * t^{\frac{1}{2}} + C_i \qquad (5)$$

$$\ln (1 - F) = -K_{LF} * t \qquad (6)$$

The IPD constant is denoted by $K_{IPD}$ (mg $g^{-1}$ $min^{-1/2}$), and the LFD constant is designated by $K_{LFD}$ ($min^{-1}$). $C_i$: the boundary layer factor, expressed as mg $g^{-1}$. The LFD plots of the BF adsorption onto $ZnAl_2O_4$, 2.5%$NiO/ZnAl_2O_4$, and 5%$NiO/ZnAl_2O_4$ composites were depicted in Fig. 11, 12, and 13, respectively. Additionally, Fig.14, 15, and 16 illustrated the IPD plots of BF sorption onto $ZnAl_2O_4$, 2.5%$NiO/ZnAl_2O_4$, and 5%$NiO/ZnAl_2O_4$, respectively. The rate-control output of BF removal (Table 3) illustrated that the LF controlled the sorption on $ZnAl_2O_4$, and 2.5%$NiO/ZnAl_2O_4$. the BF sorption onto the 5%$NiO/ZnAl_2O_4$ sorbent was controlled by the IP model.

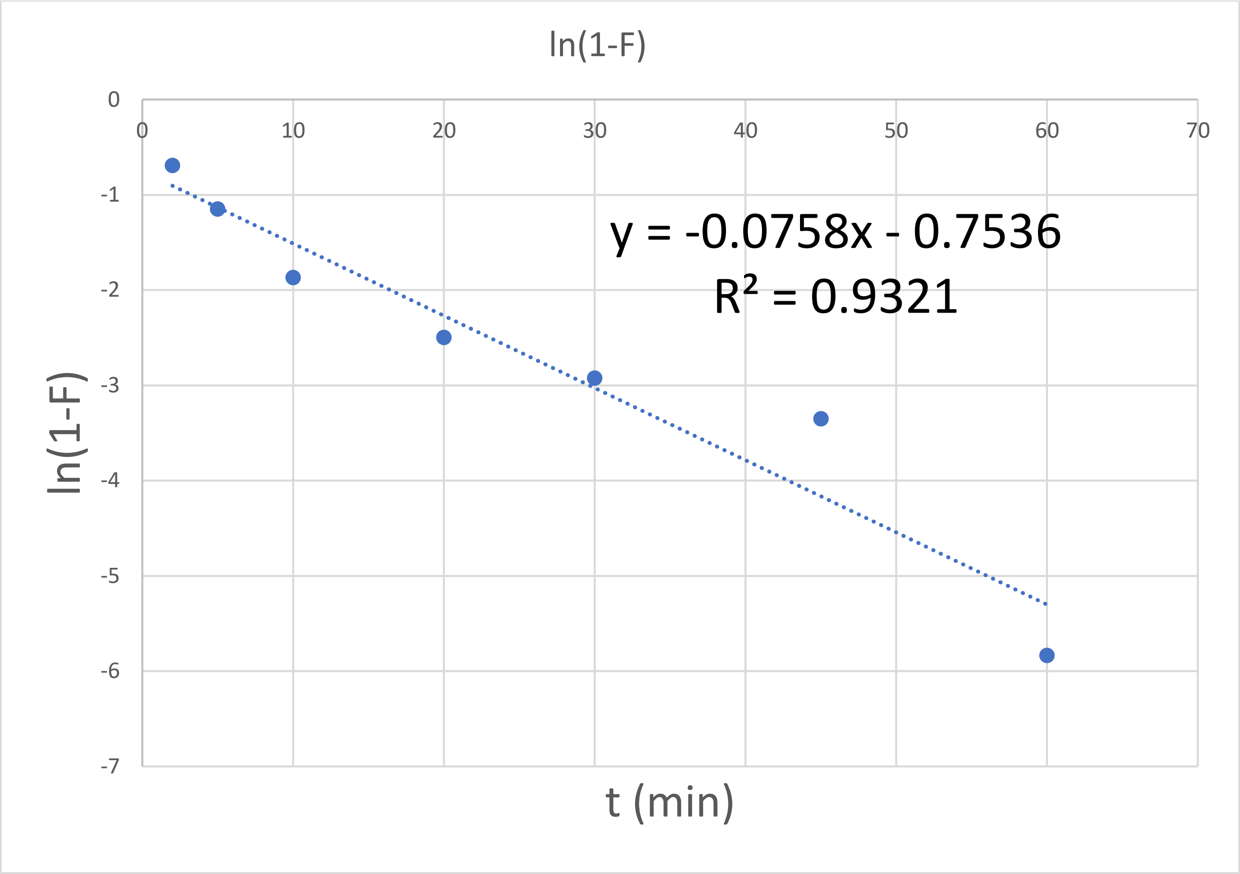

**Fig. 11 The LFD investigation of BF sorption onto $ZnAl_2O_4$ composite.**

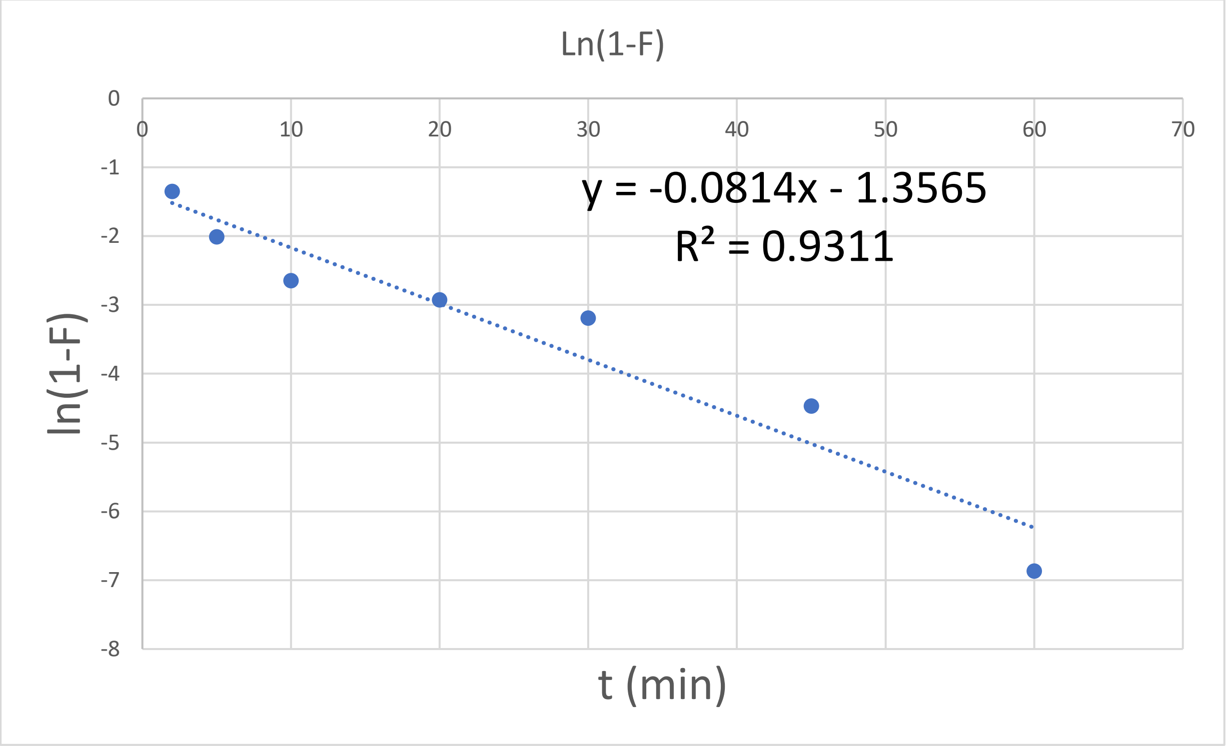

**Fig. 12 The LFD investigation of BF sorption onto 2.5%NiO/$ZnAl_2O_4$ composite.**

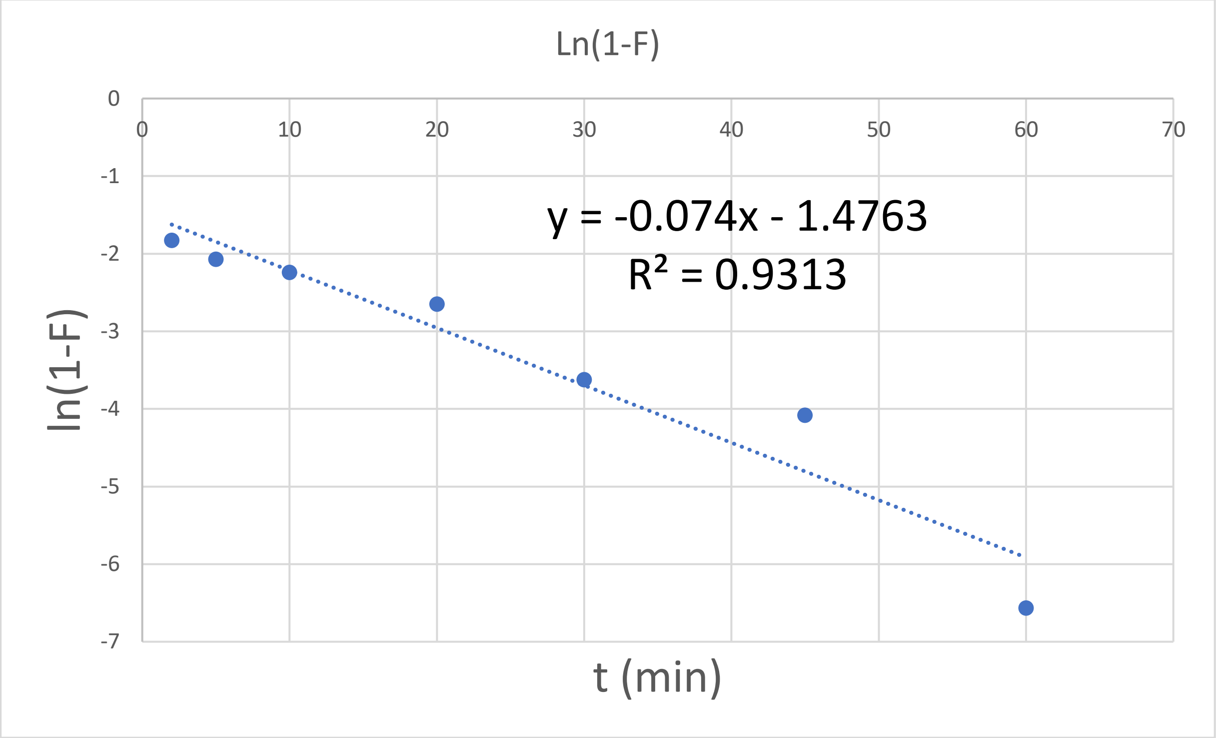

**Fig. 13 The LFD investigation of BF sorption onto 5%NiO/$ZnAl_2O_4$ composite.**

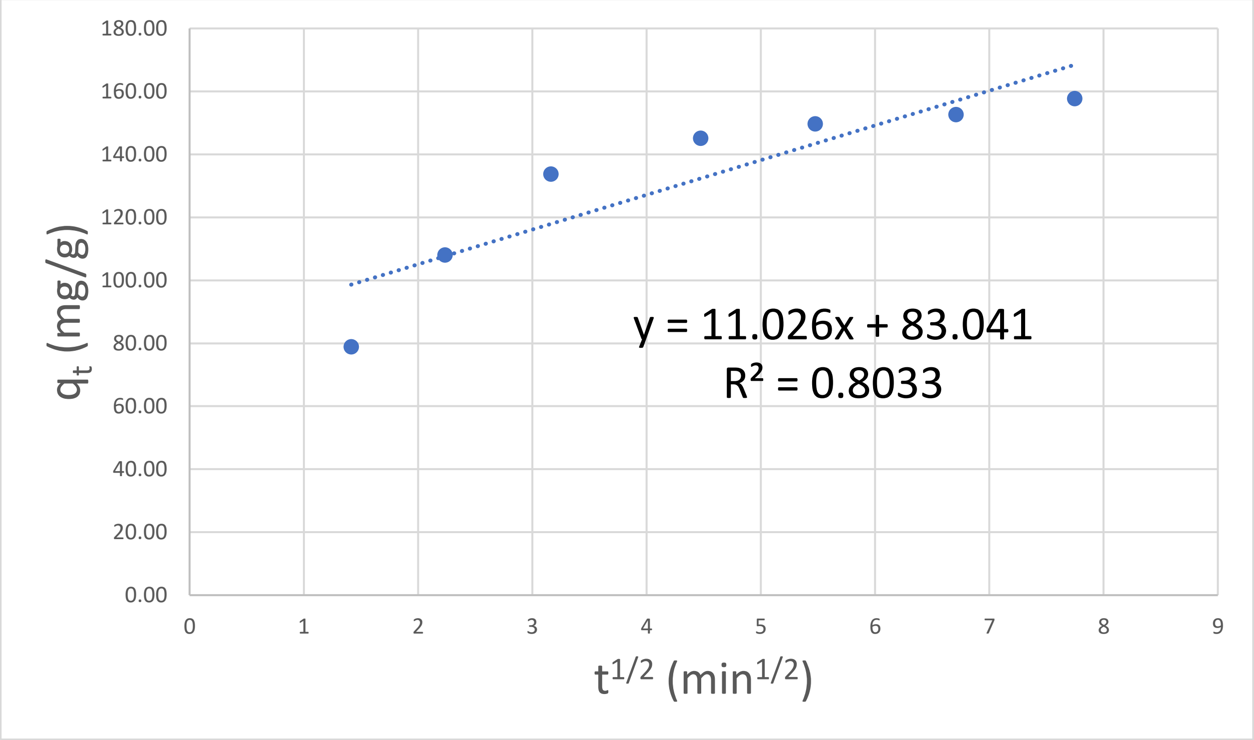

**Fig. 14 The IPD investigation of BF sorption onto $ZnAl_2O_4$ composite.**

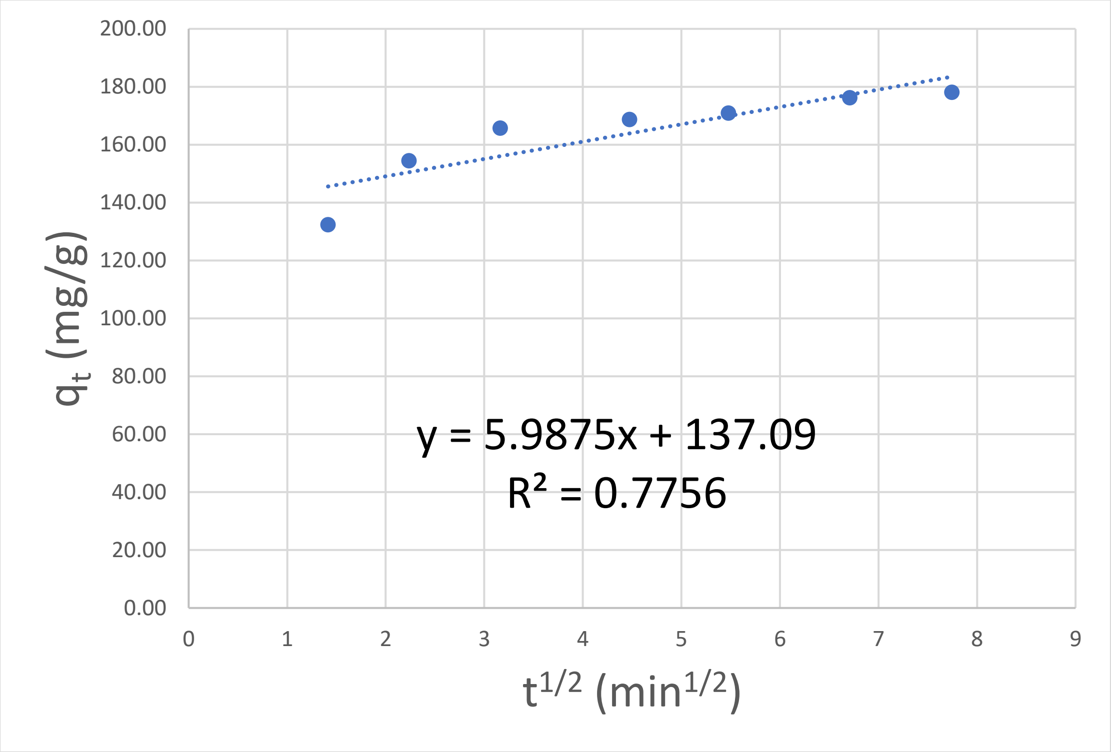

**Fig. 15 The IPD investigation of BF sorption onto 2.5%NiO/$ZnAl_2O_4$ composite.**

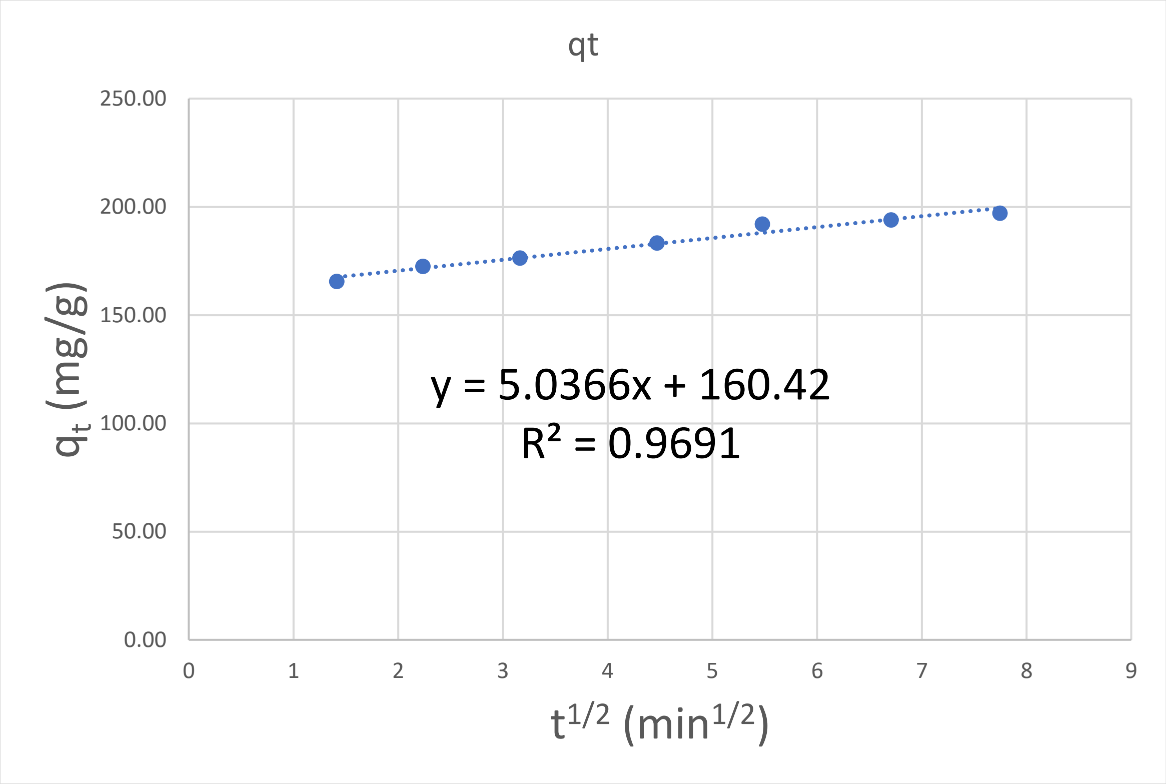

**Fig. 16 The IPD investigation of BF sorption onto 5%NiO/$ZnAl_2O_4$ composite.**

**Table 2 The adsorption rate control results of BF removal by $ZnAl_2O_4$, 2.5%NiO/$ZnAl_2O_4$, 5%NiO/$ZnAl_2O_4$, and 10%NiO/$ZnAl_2O_4$.**

| **Sorbent** | ***LFDM*** | | ***IPDM*** | |
|---|---|---|---|---|
| | **$K_{LF}$ ($min^{-1}$)** | ***$R^2$*** | **$K_{IP}$ ($mg\ g^{-1}\ min^{0.5}$)** | ***$R^2$*** |
| **AlZnO4** | **0.076** | **0.932** | **11.026** | **0.803** |
| **2.5%NiO/$AlZnO_4$** | **0.081** | **0.931** | **5.987** | **0.776** |
| **5%NiO/$AlZnO_4$** | **0.074** | **0.931** | **5.037** | **0.969** |

## 3.4. Conclusion

This study used a one-put fast method to prepare $ZnAl_2O_4$, 2.5%$NiO/ZnAl_2O_4$, and 5%$NiO/ZnAl_2O_4$ composites. The synthesized composites were studied for removing BF and from the water via adsorption. The $ZnAl_2O_4$, 2.5%$NiO/ZnAl_2O_4$, and 5%$NiO/ZnAl_2O_4$ showed $q_t$ values of 158.1, 178.3, and 197.2 mg $g^{-1}$, respectively,these results reflected that doping $ZnAl_2O_4$ by NiO improved the sorption ability of the base material. Notably, almost 90% of the gained $q_t$ values were acquired within the first 20 to 30 minutes, and all sorption processes reached equilibrium at 60 minutes, which indicated a fast treatment sorbents. The rate-order output of BF removal (Table 1) illustrated that the sorption on $ZnAl_2O_4$, and 2.5%$NiO/ZnAl_2O_4$ showed better fitting to the PS model, conversely, BF sorption onto the 5%$NiO/ZnAl_2O_4$ fitted the PF model. Additionally, the rate-control output of BF removal (Table 3) illustrated that the LF controlled the sorption on $ZnAl_2O_4$, and 2.5%$NiO/ZnAl_2O_4$. the BF sorption onto the 5%$NiO/ZnAl_2O_4$ sorbent was controlled by the IP model.

# References

1. Hasan, S.J.R.J.R.S., *A review on nanoparticles: their synthesis and types.* 2015. **2277**: p. 2502.
2. Biswas, P., C.-Y.J.J.o.t.a. Wu, and w.m. association, *Nanoparticles and the environment.* 2005. **55**(6): p. 708-746.
3. Tissue, B. and H.J.J.o.S.S.C. Yuan, *Structure, particle size, and annealing of gas phase-condensed Eu3+: Y2O3 nanophosphors.* 2003. **171**(1-2): p. 12-18.
4. Hasany, S., et al., *Systematic review of the preparation techniques of iron oxide magnetic nanoparticles.* 2012. **2**(6): p. 148-158.
5. Arole, V. and S.J.J.M.S. Munde, *Fabrication of nanomaterials by top-down and bottom-up approaches-an overview.* 2014. **1**: p. 89-93.
6. Minemoto, T., et al., *Preparation of Zn1− xMgxO films by radio frequency magnetron sputtering.* 2000. **372**(1-2): p. 173-176.
7. Ostwald, W.J.P.C., *On the Formation of Liesegang Rings.* 1897. **27**: p. 365.
8. Rayleigh, L.J.T.L., Edinburgh,, D.P. Magazine, and J.o. Science, *LXXVIII. Periodic precipitates.* 1919. **38**(228): p. 738-740.
9. Alexander, J., *Colloid Chemistry, Theoretical and Applied: Theory and methods*. Vol. 1. 1926: Chemical Catalog Company.
10. Stöber, W., et al., *Controlled growth of monodisperse silica spheres in the micron size range.* 1968. **26**(1): p. 62-69.
11. Tan, C., et al., *Production of monodisperse colloidal silica spheres: Effect of temperature.* 1987. **118**(1): p. 290-293.
12. Houshiar, M., et al., *Synthesis of cobalt ferrite (CoFe2O4) nanoparticles using combustion, coprecipitation, and precipitation methods: A comparison study of size, structural, and magnetic properties.* 2014. **371**: p. 43-48.
13. Ma, J., et al., *Preparation of cobalt ferrite nanoparticles via a novel solvothermal approach using divalent iron salt as precursors.* 2013. **48**(2): p. 214-217.
14. Tadic, M., et al., *Magnetic properties of novel superparamagnetic iron oxide nanoclusters and their peculiarity under annealing treatment.* 2014. **322**: p. 255-264.
15. Sun, C., et al., *Versatile application of a modern scanning electron microscope for materials characterization.* 2020. **55**(28): p. 13824-13835.
16. Manahan, S., *Environmental chemistry*. 2017: CRC press.
17. Ruhoy, I.S. and C.G.J.E.i. Daughton, *Beyond the medicine cabinet: an analysis of where and why medications accumulate.* 2008. **34**(8): p. 1157-1169.
18. Zhao, Y. and X. Xiao, *Environmental Antibiotics: Exposure Monitoring and Health Endpoints*, in *Emerging Chemicals and Human Health*. 2019, Springer. p. 165-178.
19. Gupta, R., B. Sati, and A. Gupta, *Treatment and recycling of wastewater from pharmaceutical industry*, in *Advances in Biological Treatment of Industrial Waste Water and their Recycling for a Sustainable Future*. 2019, Springer. p. 267-302.
20. MISHRA, R., et al., *INVESTIGATION OVER WATER QUALITY OF RIVERS GANGA AND YAMUNA DURING KUMBH-2019-A CASE STUDY AT PRAYAGRAJ (ALLAHABAD), UTTAR PRADESH, INDIA.*
21. Yihdego, Z.J.B.R.P.i.I.W.L., *The fairness 'dilemma'in sharing the Nile waters: what lessons from the grand Ethiopian renaissance dam for international law?* 2017. **2**(2): p. 1-80.
22. Verma, J., et al., *Marine pollution, sources, effect and management.* Three Major Dimensions of Life: Environment, Agriculture and Health. Prayagraj, India: Society of Biological Sciences and Rural Development, 2020: p. 270-276.
23. Sjerps, R.M., et al., *Occurrence of pesticides in Dutch drinking water sources.* 2019. **235**: p. 510-518.
24. Pan, Z., et al., *Environmental implications of microplastic pollution in the Northwestern Pacific Ocean.* 2019. **146**: p. 215-224.

25. Yadav, K.K., et al., *Fluoride contamination, health problems and remediation methods in Asian groundwater: A comprehensive review.* 2019. **182**: p. 109362.
26. Lee, H., et al., *Emergence and spread of cephalosporin-resistant Neisseria gonorrhoeae with mosaic penA alleles, South Korea, 2012–2017.* 2019. **25**(3): p. 416.
27. Gleick, P.H. and M.J.P.o.t.N.A.o.S. Palaniappan, *Peak water limits to freshwater withdrawal and use.* 2010. **107**(25): p. 11155-11162.
28. Stumm-Zollinger, E. and G.M. Fair, *Biodegradation of steroid hormones.* Journal (Water Pollution Control Federation), 1965: p. 1506-1510.
29. Daughton, C.G. and T.A. Ternes, *Pharmaceuticals and personal care products in the environment: agents of subtle change?* Environmental health perspectives, 1999. **107**(suppl 6): p. 907-938.
30. Wu, C., et al., *Water pollution and human health in China.* 1999. **107**(4): p. 251-256.
31. Chander, V., et al., *Pharmaceutical compounds in drinking water.* 2016. **6**(1): p. 5774.
32. Kairigo, P., et al., *Contamination of surface water and river sediments by antibiotic and antiretroviral drug cocktails in low and middle-income countries: occurrence, risk and mitigation strategies.* 2020. **12**(5): p. 1376.
33. Ibrahim, T.G., et al., *A Thorough Examination of the Solution Conditions and the Use of Carbon Nanoparticles Made from Commercial Mesquite Charcoal as a Successful Sorbent for Water Remediation.* Nanomaterials, 2023. **13**(9): p. 1485.
34. Almufarij, R.S., et al., *Sweep-out of tigecycline, chlortetracycline, oxytetracycline, and doxycycline from water by carbon nanoparticles derived from tissue waste.* Nanomaterials, 2022. **12**(20): p. 3617.
35. Topare, N.S. and S.A. Bokil, *Adsorption of textile industry effluent in a fixed bed column using activated carbon prepared from agro-waste materials.* Materials Today: Proceedings, 2021.
36. Yurtsever, A., et al., *Self-forming dynamic membrane bioreactor for textile industry wastewater treatment.* Science of The Total Environment, 2021. **751**: p. 141572.
37. Feng, Q., et al., *Flocculation performance of papermaking sludge-based flocculants in different dye wastewater treatment: Comparison with commercial lignin and coagulants.* Chemosphere, 2021. **262**: p. 128416.
38. Othman, M.H.D., et al., *Advanced Membrane Technology for Textile Wastewater Treatment*, in *Membrane Technology Enhancement for Environmental Protection and Sustainable Industrial Growth*. 2021, Springer. p. 91-108.
39. Chowdhury, M.F., et al., *Current treatment technologies and mechanisms for removal of indigo carmine dyes from wastewater: A review.* Journal of Molecular Liquids, 2020: p. 114061.
40. Harrache, Z., et al., *Thermodynamic and kinetics studies on adsorption of Indigo Carmine from aqueous solution by activated carbon.* Microchemical Journal, 2019. **144**: p. 180-189.
41. Oberoi, A.S., et al., *Insights into the fate and removal of antibiotics in engineered biological treatment systems: a critical review.* Environmental science & technology, 2019. **53**(13): p. 7234-7264.
42. Jones, O.A., J.N. Lester, and N.J.T.i.B. Voulvoulis, *Pharmaceuticals: a threat to drinking water?* 2005. **23**(4): p. 163-167.
43. Hussin, F., M.K. Aroua, and M.A.J.E. Kassim, *Transforming Plastic Waste into Porous Carbon for Capturing Carbon Dioxide: A Review.* 2021. **14**(24): p. 8421.